Journal of

GEOPHYSICAL RESEARCH

VOLUME 72 | APRIL 15, 1967 | No. 8

Infrasonic Waves from the Marine Storm of April 7, 1966[1]

WILLIAM L. DONN AND ERIC S. POSMENTIER

Lamont Geological Observatory, Columbia University
Palisades, New York

Nearly sinusoidal microoscillations of air pressure of the order of 1 to 10 microbars (dynes/cm²), which have been recorded on a Lamont tripartite array of line microphones, have been identified as infrasonic waves arising from an intense atmospheric low pressure system off Newfoundland. Although the nearly sinusoidal pressure variations show good coherence among the stations, there is enough wave breakdown among the stations to suggest interference from a widespread source. Other factors indicate this source to be ocean waves. It is concluded that the spectral character of both microbaroms and microseisms is a function of a common generating mechanism, but microbarom amplitude variations depend also on atmospheric conditions along the path.

INTRODUCTION

This report is concerned with a case study of atmospheric infrasonic waves, commonly known as microbaroms because of their similarity to microseisms. Such atmospheric pressure waves of about 3 to 8 sec in period and a few microbars (dynes/cm²) in amplitude were originally described by *Benioff and Gutenberg* [1939], *Gutenberg and Benioff* [1941], and *Baird and Banwell* [1940], who observed pressure fluctuations closely related to times of microseism activity at Pasadena, California, and Christchurch, New Zealand, respectively. Further research, particularly by *Saxer* [1945, 1954], *Dessauer et al.* [1951], *Daniels* [1953, 1962], and *Cook* [1962*a, b*], confirmed the relationship of microbaroms to marine storms and emphasized an origin from ocean waves. Most of the investigations noted a similarity in the activity of microbaroms and microseisms, although the microbaroms showed a diurnal variation, with intensity being most pronounced at night. Seasonal variations for both microbaroms and microseisms show a peak in winter. *Saxer* [1954] explained diurnal and seasonal variations of microbarom intensity on the basis of temperature and wind currents in the lower 50-km layer of air, but the fundamental cause of the winter intensification is more probably the winter increase of marine storms.

There is still considerable uncertainty about the origin and propagation of microbaroms partly because of a lack of systematic empirical data. The correlation between the activities of microseisms and microbaroms has led us to extend our investigation of air pressure waves into this range, in view of the large seismological installation and record collection at Lamont. Our previous studies here have been related to atmospheric internal gravity waves of about 2 to 12 min in period and acoustic-gravity waves from explosive sources in the same period range.

INSTRUMENTATION

The microbarom detection system is a tripartite array of line microphones located in

[1] Lamont Geological Observatory Contribution 1028.

Tallman State Park and Collins property, both near Lamont. The array, shown in Figure 1, is nearly a right triangle with sides of 577, 789, and 988 meters. Their lengths are, thus, approximately half the anticipated typical wavelength. This gives time lags long enough for the accurate calculation of wave vectors, yet short enough to avoid ambiguity in matching the three wave records. In a fairly complete discussion of the directional resolving power of different types of arrays of wave detectors, *Barber* [1963] showed that the optimum component separation in a triangular array is about half the wavelength. Each of the three line microphones used consists of an LTV (Ling Temco Vought) condenser microphone in a noise-reducing pipe oriented as shown in Figure 1.

The sensitive element of the microphone is a small stainless steel diaphragm that is part of a balanced capacitance bridge circuit. The reference or back volume and back leak are adjusted to have a response that is nearly flat from audible frequencies down to 0.1 cps (10-sec period); the over-all response typical of the three instruments is shown in Figure 2.

Because microbarom periods are in the same range as pressure noise from the local small wind eddies that travel with the ambient wind speed rather than with acoustic speed, the Daniels-type noise-reducing pipe [*Daniels*, 1959] was used to improve the signal-to-noise ratio. Each noise-reducing unit is a 1000-foot straight pipe, with small capillary openings to the atmosphere every 10 feet. The pipe tapers symmetrically in stages from a 2-inch plumbing size at its center, where the microphone is mounted, to $\frac{3}{8}$-inch size at its ends. Each reduction in diameter is calculated to match the parallel combination of the resistance of the capillary and the impedance of the smaller pipe section with the impedance of the larger pipe section. The pipe is thus nonreflecting for propagation away from its center or away from the microphone. The 10-foot capillary spacing is based on an estimate of the smallest size of the local wind eddies.

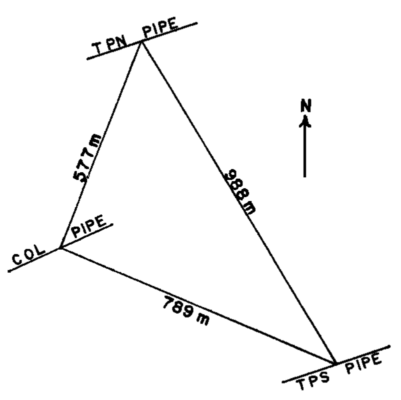

Fig. 1. The Lamont Geological Observatory infrasonics array of line microphones.

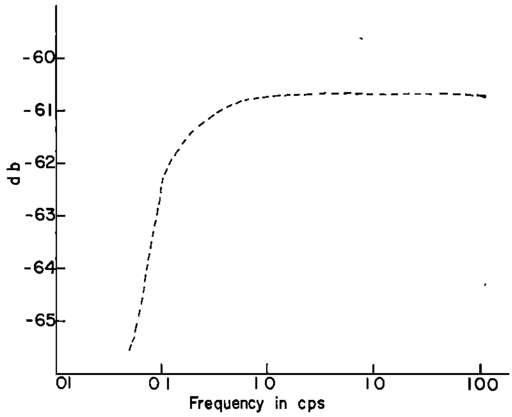

Fig. 2. Response curve of the LTV condenser microphone.

Signals that travel at acoustic speeds parallel to the pipe or that have wavelengths large compared with the pipe will enter each capillary and add coherently (in amplitude) at the center of the pipe, whereas subacoustic signals with small wavelengths (such as pressure fluctuations from slow wind eddies) will add incoherently (in power). An acoustic signal with amplitude A, being received by a pipe with N openings, will produce a net amplitude NA or a power $(NA)^2$. A subacoustical signal of small wavelength and amplitude B, would produce a net power of $N(B^2)$. The ratio of the two powers would thus be increased by a factor of N from A^2/B^2 to N^2A^2/NB^2. The kind of noise reduction provided by this system is illustrated in Figure 3, which compares simultaneous recordings by adjacent microphones, one of which is in a noise-reducing pipe. At times of low noise both signals are identical, indicating that no signal attenuation is introduced by the pipe. The pipe is effective at moderate wind velocities, as illustrated. When wind speeds become strong—

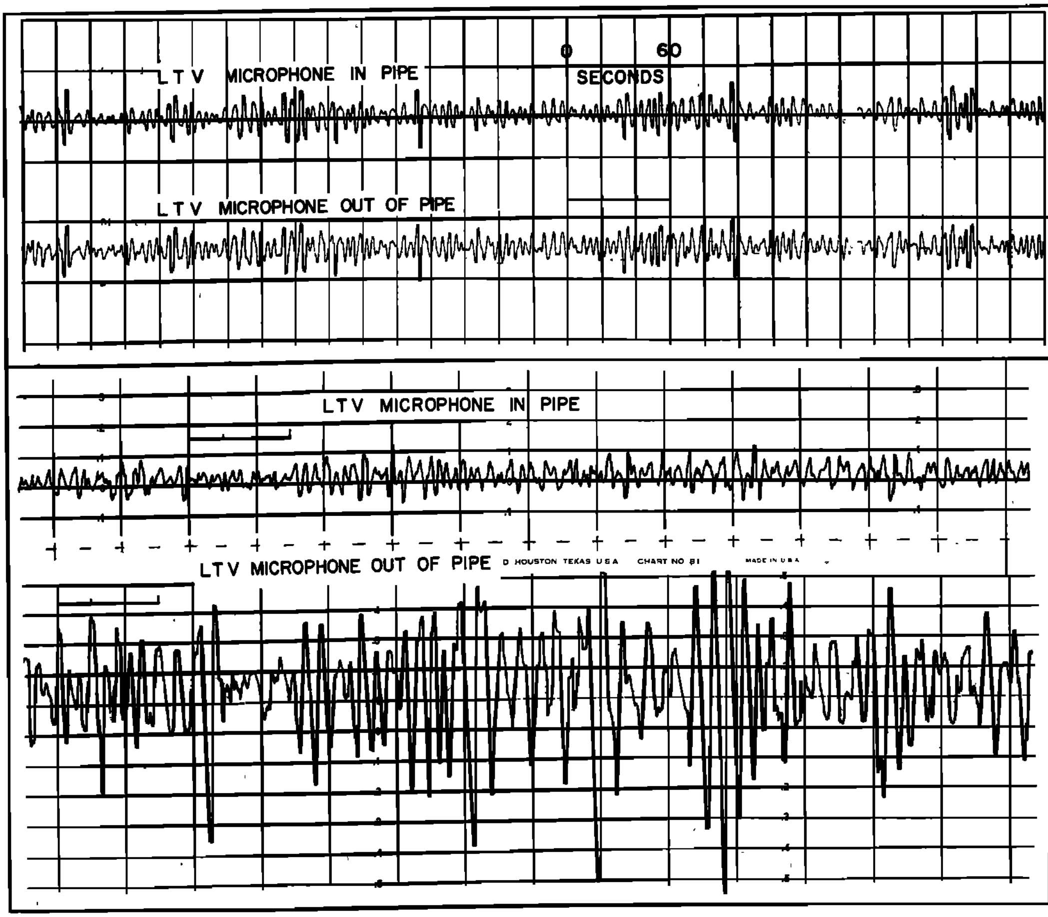

Fig. 3. Comparison of pressure recorded by microphones with and without a noise-reducing pipe, on a quiet day (top) and a moderately windy day (bottom).

20 or more mph—noise level becomes too high for operational use of visual records even with a noise-reducing system.

A double-ended pipe of the type described is essentially omnidirectional for wavelengths in the microbarom range. Signals from the pipe array are telemetered without FM conversion over leased telephone lines to the laboratory, where further electronic filtering is used, primarily to remove the strong long-period noise that would not be suppressed by the acoustic pipes. Recording is now continuous on analog magnetic tape with continuous visual monitoring on seismic-type drum recorders.

Data

Nature of the signal. The Lamont infrasonic array of microbarographs has not been in operation long enough for the compilation of data for the statistical analysis of time variations of amplitude and period, such as those referred to in the introduction. The few cases of high microbarom activity that have occurred with very low noise level have, however, facilitated study and allowed unambiguous data analysis. One such clear-cut case was the microbarom-microseism storm of April 7, 1966.

Figure 4 shows the simultaneous recordings at about 0600 GMT of microseisms from a Lamont vertical component seismometer (T_0: 15 sec; electronic, broad band response) and the three microbarographs indicated. All the traces show relatively noise-free signals which visually appear almost identical in period. The three pressure records possess a similar pattern and wave form, indicating good coherence over

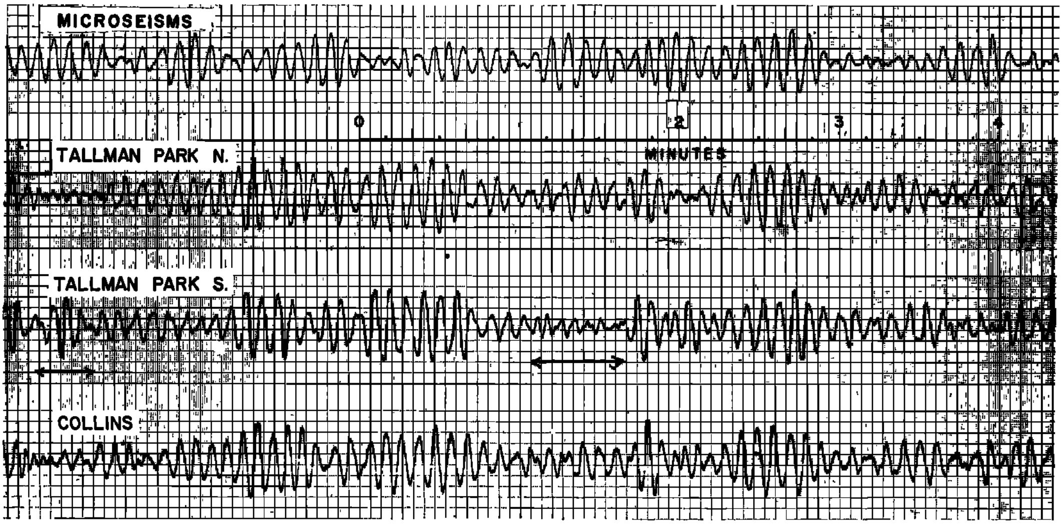

Fig. 4. Microbaroms recorded by the tripartite network on April 7, 1966, 0600 GMT and concurrent microseisms. (Note that polarity is reversed on Tallman Park S.)

the tripartite array. (Note that the polarity on the Tallman Park S instrument is reversed.) The microbarom records show wave envelopes that are strikingly similar to the beat patterns characteristic of microseisms.

Despite the generally good coherence, some inconsistencies exist among the three pressure traces. In Figure 4, to the left of the word 'minutes' coherence is good between Tallman Park N and Collins but breaks down on Tallman Park S, as indicated just above the arrow. Farther to the left, below the 'T,' the strong wave group in the Tallman Park S recording does not appear with clear definition on either of the other two traces. These examples show wave breakdown in a direction that will be shown later to be along the wave crests. Among the three stations of the array, coherence was usually best between Tallman Park N and Collins.

Spectrum analysis. In our data analysis, the magnetic-tape signals are transferred to a tape loop in the Noratom Isac (Instrument for Statistical Analog Computation), which is used for the computation of power spectra and cross-correlation functions. Spectra were computed for microbaroms and microseisms from signal samples of 30-min duration at 0000, 0600, and 1200 GMT, for this case. The actual machine printout results are illustrated in Figure 5, in which power is plotted in arbitrary units on a linear scale and period is plotted on a hyperbolic scale (relabelled from the original linear frequency scale). The three microbarom spectra are shown to one power scale, and the microseism spectra are shown to another.

As was apparent in the visual records, the spectral peaks of microbaroms and microseisms are strikingly close in period. Actually, the microseism spectral bands appear to be shifted toward longer periods by about ½ sec, or slightly less. The spectra of both microbaroms and microseisms show split peaks at about the same period and interesting small side peaks. The individual peaks remain unchanged in period over the 12-hour interval despite the large amplitude variations in the case of the microbaroms. Note, for example, the microbarom peaks at 5.8 and 6.3 sec and the microseisms peaks at 5.9 and 6.5 sec. For the microseisms the distribution of power shifts to the longer period peaks during the 12 hours.

At the time of this case, recording was programmed for 30-min intervals every 6 hours. Both the records and the spectra show a strong increase in microbarom amplitude from 0000 to 0600 (when double amplitudes reached several microbars) and a strong partial decrease by 1200. In contrast, microseisms remained at about the same high level during the 12-hour

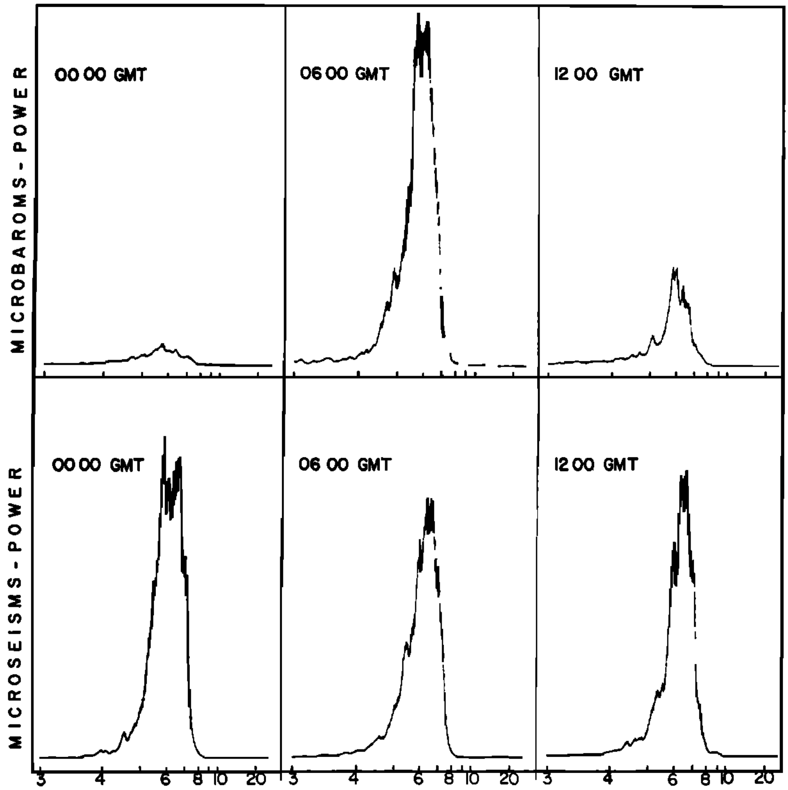

Fig. 5. Microbarom and microseism power spectra.

interval. Despite the difference in amplitude variations, the dominant periods of both types of signals coincided, as noted above.

Wave vectors and synoptic data. In order to determine wave directions and speeds, the time lags among the three microphone stations were measured from the cross-correlation functions computed and printed out by the Isac. An example of the correlation functions and measurement of the time lag for Tallman Park S and Collins is shown in Figure 6. The sinusoidal shape of the cross-correlation functions and the small decrease in correlation coefficient from the central to the adjacent peaks show the purity of the wave forms, as already manifested in the records and spectra.

Wave coherence among the three channels was judged too poor at the time of relatively low amplitude at 0000 to permit the determination of a reliable vector. At 0600 wave arrival was from N58°E with a horizontal speed of 339.6 m/sec (1114 ft/sec). At 1200 the arrival direction was N52°E, and the horizontal speed 338.7 m/sec (1111 ft/sec). These directions, which are drawn on the synoptic surface weather charts in Figure 7, indicate clearly that the waves came from the direction of a large intense low pressure area located off northeastern North America.

At present, Lamont does not operate a local tripartite seismic station, but approximate microseism vectors can be determined by phase

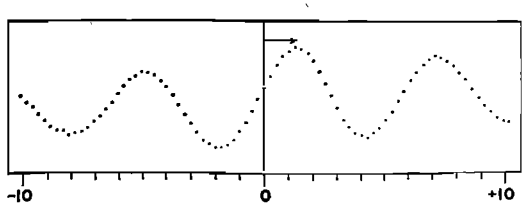

Fig. 6. Cross-correlation of the Tallman Park S and Collins records. The abscissa gives the time by which Collins signal lags Tallman Park S signal.

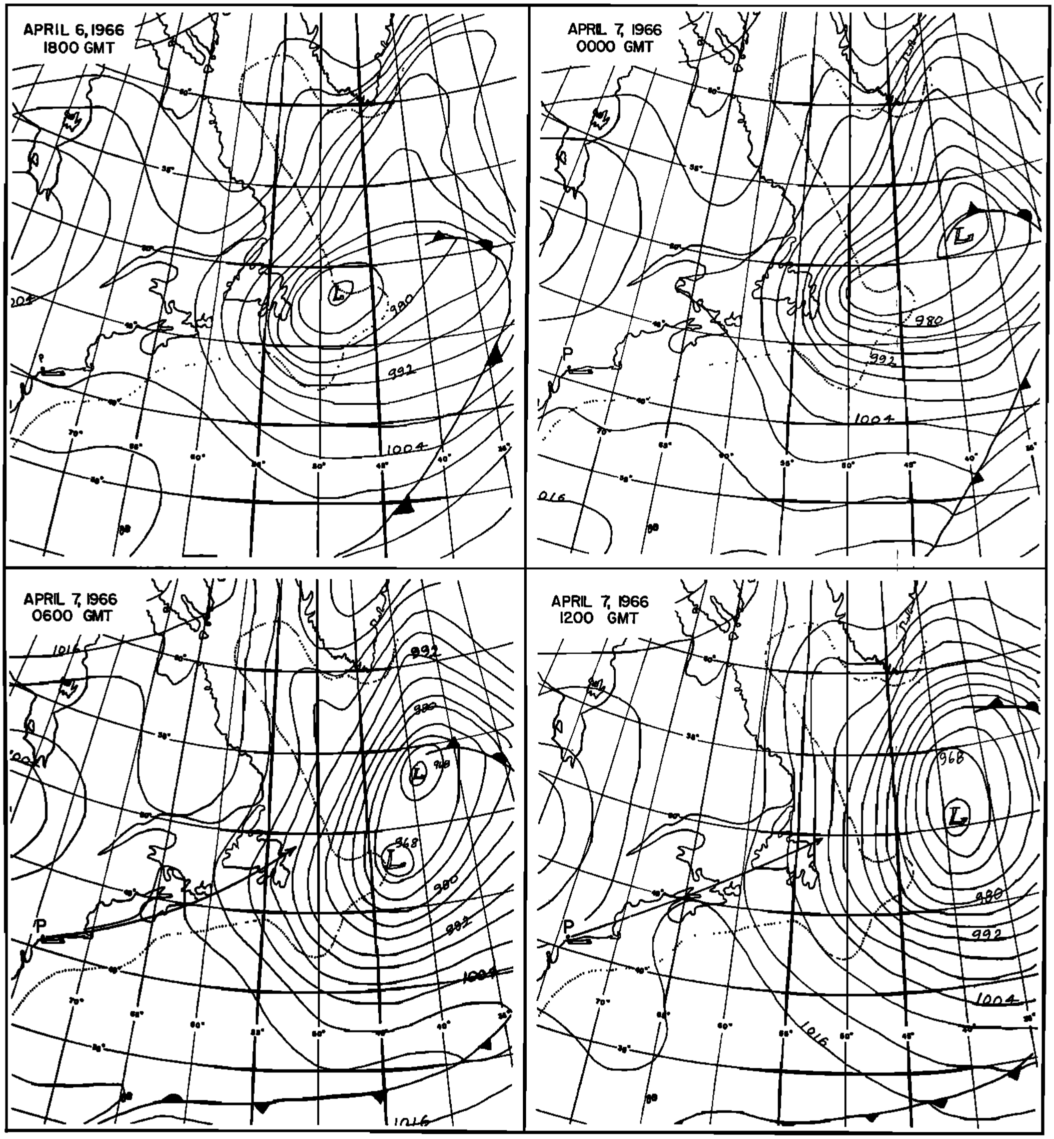

Fig. 7. Surface synoptic charts having the directions of arrival of microbaroms and the low pressure system indicated as the source for both mircobaroms and microseisms.

comparison among the three seismograph components, if we accept the microseisms as having typical Rayleigh wave ground particle motion. Arrival directions from the northeast quadrant were obtained through this procedure. The same storm is clearly related to both microseisms and microbaroms.

The storm itself is of interest here because it developed to maximum size and strength over a 24-hour period, while its area of strong wind motion remained nearly stationary.

Discussion

The wave vector at both 0600 and 1200 indicates, according to Figure 7 and 8, the mean positions of several regions of the storm as possible microbarom sources: (1) the part of the storm nearest the recording station, (2) the most intense part of the storm, (3) the coastal region affected by the highest storm waves, and (4) the region of steepest wave height gradient, as well as (5) the large area of storm winds

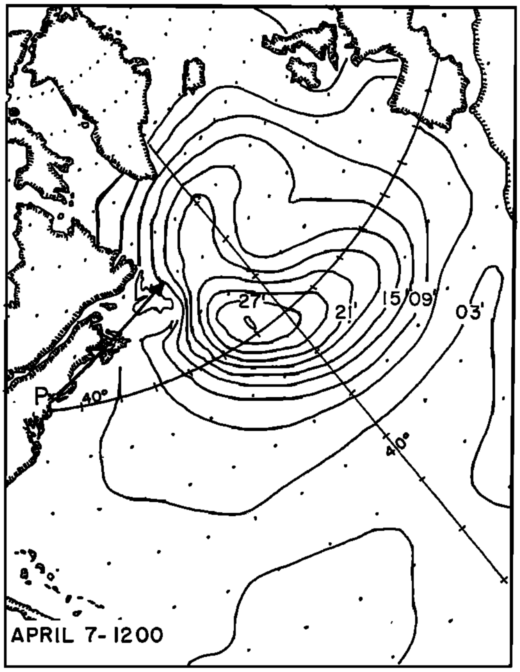

Fig. 8. Sea height analysis for the storm of April 7, 1966, as prepared at the U. S. Fleet Weather Central. Height contours are drawn at 3-foot intervals. The microbarom vector for 1200 GMT is also shown.

and (6) the large area of high storm waves (greater than 12 feet). Comparison with ocean waves at the time of strong microbarom activity at 0600 GMT is not possible because of the wave analysis schedule (0000 and 1200 GMT). However, the height pattern changed little between these times.

If the origin of the microbaroms is related to items 1 to 4, above, the angular spread of the source should be small. If their origin is related to a mechanism involving a larger storm area, the angular spread of the source should be relatively large. On the basis of the meteorological parameters in Figure 7, the source for item 5 is about 40°, on the basis of the wave diagram in Figure 8, the angle for item 6 is about 45°.

The information about the wave pattern and coherence of the microbaroms can help resolve the ambiguity in their source among items 1 to 6. We noted earlier that microbaroms occur in beat patterns similar to the pattern of microseisms, and that a certain breakdown in coherence occurred over the network whose dimensions are about one-half the microbarom wavelength. A similar lack of coherence [*Donn and Blaik*, 1953] for microseisms traversing a tripartite network has been explained by them as the result of interference of waves arriving from a large source or from more than one storm source.

In the present case no other reasonable atmospheric disturbance exists to act as an additional generating area for the observed microbaroms. Interference of waves approaching from a random source distribution within a relatively large generating area thus appears to be the cause of the beats and the occasional breakdown in coherence.

To determine the actual coherence between microphones of Tallman Park N and Tallman Park S (approximately one-half wavelength apart along the crest line), the Isac was used to measure the amplitudes of their cross-correlation function. The value at maximum correlation, which is taken to be the coherence of the two signals, is 0.80.

The theoretical coherence between signals observed at two points along the crest line of waves from broad sources has been discussed theoretically by Posmentier (in preparation). Figure 9 shows the results for different station separations for two microphones and the circular arc source illustrated in the inset. A coherence of 0.80 is the calculated result for a microphone separation of one-half wavelength and a source spread of 42°. The source, in the calculations, was assumed to remain constant in period and amplitude over the entire arc θ

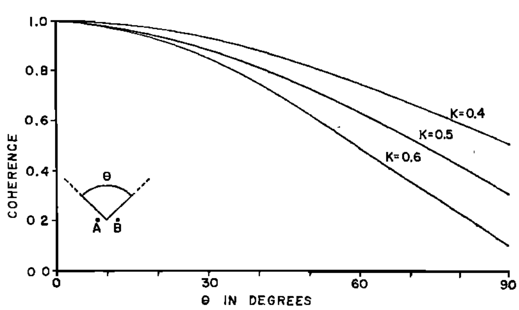

Fig. 9. Correlation coefficient of signals at adjacent receivers as a function of source angle for three values of K (receiver separation/wave length). The inset shows the geometry of the assumed source and receivers (A and B).

and constant in time, but with random phase relationships among points on the arc.

If the lack of microbarom coherence is interpreted as the effect of a broad sector of arrivals, this analysis favors their origin from ocean waves operating over a large area as opposed to an origin related to items 1 to 4 above. Item 5, the region of high storm winds, is eliminated because it is not unique to marine storms, the only kind known to generate microbaroms. An ocean wave mechanism has generally been assumed for microbarom origin, but the method of coupling the wave energy to the atmosphere has been treated very differently in each investigation. In a relatively large storm area, the realistic sea surface consists of fluctuating wave envelopes and interfering waves whose net pressure field is of the correct order of magnitude necessary to produce microbaroms of the amplitude and period observed (Posmentier, in preparation).

The location and extent of the generating area are clearly of importance in understanding the coupling mechanism. Because a single tripartite array can provide only a single vector or arrival direction, we plan to install at least one more such array at an appropriate remote location in order to improve our determination of these parameters.

Our recording program of ½ hour every 6 hours, at the time of this case, prevented a clear documentation of the time variations of amplitude. Maximum recorded amplitudes occurred about 0600, the microbarom intensity having been much less at the preceding 0000 and the following 1200 GMT recording times. During this 12-hour interval, at least, microseism amplitudes were at a continuously high level as was the generating storm off Newfoundland. There is nothing in the synoptic charts of storm or wave characteristics that suggests the presence of any special generating conditions about 0600, April 7, or that indicates generation of both microbaroms and microseisms was not continuous during, at least, the 12-hour period of observation. *Baird and Banwell* [1940] and *Saxer* [1954] described a diurnal variation in microbarom amplitude with maximum intensities occurring at night. Saxer ascribed this to the wind currents and temperature changes in the layer of air 50 km up. The importance of propagation effects seems to be supported by this case. The audibility of microbaroms may well be determined by the geometry of the acoustic-ray paths between source and observer.

The lack of correlation between microseism and microbarom amplitude fluctuation just described indicates that microbaroms are not generated by the microseismic local ground motion, or the ground motion along the propagation path. *Cook* [1962*a*] reached a similar conclusion on the basis of the amplitude of atmospheric pressure fluctuations which he calculated would result from microseismic ground motion.

The similarity in period and in period variations of microbaroms and microseisms, which is one of the most striking features of this storm and others we have studied, has also been observed by other investigators. For example, *Baird and Banwell* [1940] found that the period of air pressure oscillations agreed with the period of concurrent microseisms. Since the phenomena are not coupled, the observed correlation between microbarom and microseism periods indicates that period is determined by characteristics of a common generating mechanism, rather than by their respective propagating media.

Acknowledgments. F. Witt installed and maintained the microphone array that provided the data for this report.

This research was supported in full by NSF grants GP 2860 and GP 5136 to Columbia University.

References

Baird, H. F., and C. J. Banwell, Recording of air-pressure oscillations associated with microseisms at Christchurch, *New Zealand J. Sci. Technol.*, *21B*, 314–329, 1940.

Barber, N. F., The directional resolving power of an array of wave detectors, in *Ocean Wave Spectra,* Proc. of a Conference sponsored by the U. S. Naval Oceanographic Office and the National Academy of Sciences 1961, pp. 137–150, Prentice-Hall, Englewood Cliffs, N. J., 1963.

Benioff, H., and B. Gutenberg, Waves and currents recorded by electromagnetic barographs, *Bull. Am. Meteorol. Soc.*, *20*, 421–426, 1939.

Cook, R. K., Strange sounds in the atmosphere, 1 and 2, *Sound, 1*(2) and (3), 1962*a*.

Cook, R. K., Radiation of sound by ocean waves, *Fourth Intern. Congr. Acoustics,* 1962*b*.

Daniels, F. B., The mechanism of generation of infrasound by the ocean waves, *J. Acoust. Soc. Am.*, *25*, 796, 1953.

Daniels, F. B., Noise-reducing line microphone for frequencies below 1 cps, *J. Acoust. Soc. Am.*, *31*, 529–531, 1959.

Daniels, F. B., Generation of infrasound by ocean waves, *J. Acoust. Soc. Am.*, *34*(3), 352–353, 1962.

Dessauer, F., W. Graffunder, and J. Schaffhauser, Über atmosphärische Pulsationen, *Arch. Meteorol. Geophys. Bioklimatol., A*, *3*, 453, 1951.

Donn, W. L., and M. Blaik, A study and evaluation of the tripartite seismic method of locating hurricanes, *Bull. Seismol. Soc. Am.*, *43*, 311–329, 1953.

Gutenberg, B., and H. Benioff, Atmospheric pressure waves near Pasadena, *Trans. Am. Geophys. Union*, *22*, 424–426, 1941.

Saxer, L., Electrische Messung kleiner atmosphärischer Druckschwankingen, *Helv. Phys. Acta.*, *18*, 527, 1945.

Saxer, L., Über Entstehung und Ausbreitung quasiperiodischer Luftdruckschwankungen, *Arch. Meteorol. Geophys. Bioklimatol., A*, *6*, 451, 1954.

(Received September 9, 1966.)